Title	Enhancement of maximum attainable ion energy in the radiation pressure acceleration regime using a guiding structure
Author(s)	Bulanov S. S., Esarey E., Schroeder C. B., Bulanov S. V., Esirkepov T. Z., Kando Masaki, Pegoraro F., Leemans W. P.
Citation	Physical Review Letters, 114(10), p.105003_1-105003_5
Text Version	Publisher's Version
URL	https://jopss.jaea.go.jp/search/servlet/search?5050652
DOI	https://doi.org/10.1103/PhysRevLett.114.105003
Right	© 2015 American Physical Society

Enhancement of Maximum Attainable Ion Energy in the Radiation Pressure Acceleration Regime Using a Guiding Structure

S. S. Bulanov,[1] E. Esarey,[2] C. B. Schroeder,[2] S. V. Bulanov,[3,4,5] T. Zh. Esirkepov,[3] M. Kando,[3] F. Pegoraro,[6] and W. P. Leemans[1,2]

[1]*University of California, Berkeley, California 94720, USA*
[2]*Lawrence Berkeley National Laboratory, Berkeley, California 94720, USA*
[3]*Kansai Photon Science Institute, JAEA, Kizugawa, Kyoto 619-0215, Japan*
[4]*Prokhorov Institute of General Physics, Russian Academy of Sciences, Moscow 119991, Russia*
[5]*Moscow Institute of Physics and Technology, Dolgoprudny, Moscow Region 141700, Russia*
[6]*Physics Department, University of Pisa and Istituto Nazionale di Ottica, CNR, Pisa 56127, Italy*

(Received 30 October 2013; revised manuscript received 17 June 2014; published 13 March 2015)

Radiation pressure acceleration is a highly efficient mechanism of laser-driven ion acceleration, with the laser energy almost totally transferrable to the ions in the relativistic regime. There is a fundamental limit on the maximum attainable ion energy, which is determined by the group velocity of the laser. In the case of tightly focused laser pulses, which are utilized to get the highest intensity, another factor limiting the maximum ion energy comes into play, the transverse expansion of the target. Transverse expansion makes the target transparent for radiation, thus reducing the effectiveness of acceleration. Utilization of an external guiding structure for the accelerating laser pulse may provide a way of compensating for the group velocity and transverse expansion effects.

DOI: 10.1103/PhysRevLett.114.105003 PACS numbers: 52.25.Os, 52.27.Ny, 52.38.Kd

Laser acceleration of charged particles is conceived to be one of the main applications of many powerful laser facilities that are being projected, built, or already in operation around the world. Ultrashort electromagnetic pulses provided by these facilities are able to generate very strong accelerating fields in a plasma, which exceed those of the conventional accelerators by orders of magnitude. This potentially opens a way for compact or even tabletop future accelerators providing beams of charged particles ranging from several MeV to multi GeV for many applications [1–3]. In particular, the laser accelerated ion beams can be used in fast ignition [4], hadron therapy [5], radiography of dense targets [6], injection into conventional accelerators [7], and nuclear physics [8].

There is a wide variety of mechanisms of laser ion acceleration depending on the design of the laser matter interaction, ranging from solid density foils to clusters and gas targets, from long to ultrashort pulses, and from 10^{18} W/cm^2 to 10^{22} W/cm^2 peak laser intensities [3]. Theoretical studies of laser ion acceleration show that radiation pressure acceleration (RPA) [9] is one of the most efficient mechanisms of acceleration [9,10], and several recent experiments may indicate the onset of this mechanism in laser-thin foil interactions [11]. RPA is based on the relativistic mirror concept [12]: the laser pulse, reflected back by the receding mirror, pushes the mirror forward. The role of the mirror in the laser-plasma interaction is played either by an ultrathin solid density foil or by plasma density modulations emerging when the laser pulse interacts with an extended undercritical density target, the so-called hole-boring RPA [13,14].

The relativistic mirror concept dates back to the paper by Einstein [15] on special relativity, where it was mentioned as an example of the relativistic effects in the light reflection by the moving mirror. If the laser is reflected by a mirror moving in the same direction with a relativistic velocity, then the reflected radiation would have the frequency downshifted by a factor of $(1-\beta^2)/(1+\beta^2) \approx 1/(4\gamma^2)$ for $\gamma \gg 1$, where β is the velocity of the mirror, normalized to the speed of light in vacuum, and γ is the mirror Lorentz factor. The energy transferred to the mirror by the laser can be estimated as $[1-1/(4\gamma^2)]\mathcal{E}_L$ for $\gamma \gg 1$, where $\mathcal{E}_L$ is the energy of the laser pulse, and for $\gamma \gg 1$ almost all laser energy can be transferred to the mirror. However, the effects of the electromagnetic (EM) wave group velocity being smaller than the vacuum speed of light were not taken into account when deriving the scaling for the RPA mechanism. A group velocity less than the vacuum light speed naturally appears in the case of focused EM radiation or when EM radiation propagates in a guiding structure or medium. It is well known that group velocity effects play a major role in laser-driven electron acceleration [1] and should naturally modify the RPA [14]. The frequency downshift of such an EM wave reflected by a receding relativistic mirror is $\omega_r = \omega[1-2\gamma^2\beta(\beta_g-\beta)]$, where ω and ω_r are the frequency in the incident and reflected EM wave, $\beta_g = v_g/c$ with v_g being the laser pulse group velocity. The energy transferred from the pulse to the mirror is

$$\Delta\mathcal{E} \simeq 2\gamma^2\beta(\beta_g - \beta)\mathcal{E}_L. \quad (1)$$

If $\beta = \beta_g$, then there is no interaction of the laser light with the target. Thus, the group velocity of the pulse limits the value of the attainable velocity of the foil.

As mentioned above, tightly focused laser pulses have group velocities smaller than the vacuum light speed, and, since they offer the high intensity needed for the RPA regime, it is plausible that group velocity effects would manifest themselves in the experiments involving tightly focused pulses and thin foils. However, in this case, finite spot size effects [16] are important and another limiting factor, the transverse expansion of the target, comes into play that may dominate over the group velocity effect. As the laser pulse diffracts after passing the focus, the target expands accordingly due to the transverse intensity profile of the laser. Due to this expansion, the areal density of the target decreases, making it transparent for radiation and effectively terminating the acceleration. The finite reflectivity of the foil greatly affects the effectiveness of the RPA mechanism [17–20].

In what follows, we study the RPA of a thin solid density foil by an EM wave with group velocity less than the speed of light in vacuum, $\beta_g < 1$. In the ultrarelativistic case, the energy of ions tends to $\mathcal{F}_L/n_e l$, where $\mathcal{F}_L$ is the laser pulse fluence (incident laser energy per unit area) and $n_e l$ is the areal density of the foil with n_e being the electron foil density and l being the foil thickness [9]. The maximum ion energy is determined by the peak laser fluence, $\max[\mathcal{F}_L]$. As shown below, in the case when $\max[\mathcal{F}_L]/n_e l > \gamma_g = (1-\beta_g^2)^{-1/2}$, the group velocity limits the maximum attainable ion energy to γ_g. We also study the RPA of a thin foil by a diffracting laser pulse and the termination of the acceleration due to increasing transparency of the expanding foil. We show that these two limitations can be mitigated by the utilization of an external guiding structure: the acceleration inside the self-generated channel in the near critical density (NCD) plasma tends to produce ion beams with higher energies.

In the RPA mechanism of laser ion acceleration, the force acting on a foil is expressed in terms of the flux of the EM wave momentum [9], which is proportional to the Poynting vector, $\mathbf{S} = \mathbf{E}\times\mathbf{B}/4\pi$. For a circularly polarized wave, the vector potential is $\mathbf{A} = A_0(\mathbf{e}_y\cos\varphi + \mathbf{e}_z\sin\varphi)$, $\varphi = \omega t - kx$, where k is the wave vector, and the Poynting vector is $\mathbf{S} = \omega k A_0^2\mathbf{e}_x$. In a frame of reference moving with the foil, the product of wave frequency $\bar{\omega}$ and wave vector $\bar{k}$ is given by [14]

$$\bar{\omega}\,\bar{k} = \omega^2\frac{(\beta_g - \beta)(1-\beta\beta_g)}{1-\beta^2}. \quad (2)$$

In this reference frame, the sum of the EM wave fluxes gives rise to the force acting on the foil: $(1 + |\rho|^2 - |\tau|^2)\mathbf{S}$, where ρ and τ are the reflection and transmission coefficients of the foil in the rest frame of reference. These coefficients enter the energy conservation relation, $|\rho|^2 + |\tau|^2 + |\alpha|^2 = 1$, where α is the absorption coefficient. Using these relationships, we can write the equation of motion for the on-axis element of the foil, which depends on the peak fluence, to obtain the maximum ion energy [14],

$$\frac{d\beta}{d(\omega t)} = \kappa\beta_g(1-\beta^2)^{1/2}(\beta_g - \beta)(1-\beta\beta_g), \quad (3)$$

where

$$\kappa = (2|\rho|^2 + |\alpha|^2)\frac{\omega A_0^2}{4\pi n_e l m_i} = \frac{1}{2}(2|\rho|^2 + |\alpha|^2)\frac{m_e}{m_i}\frac{a^2(\varphi)}{\varepsilon_e}. \quad (4)$$

Here, $a = eA/m_e c^2$ is the normalized laser pulse amplitude, $\varepsilon_e = \pi(n_e l/n_{\rm cr}\lambda)$ is the parameter governing the transparency of the thin solid density target [21], λ is the laser wavelength, $n_{\rm cr} = m_e\omega^2/4\pi e^2$ is the critical plasma density, e and m_e are the electron charge and mass, respectively, n_e is the electron density in the foil, and m_i is the ion mass. Equation (3) can be solved in quadratures,

$$\left\{\ln\frac{(1-\beta\beta_g + (1-\beta_g^2)^{1/2}(1-\beta^2)^{1/2}\beta_g}{(\beta_g-\beta)(1+(1-\beta_g^2)^{1/2})} - \beta_g\left[\arctan\frac{(1-\beta_g^2)^{1/2}(1-\beta^2)^{1/2}}{\beta_g - \beta} - \arccos\beta_g\right]\right\} = \beta_g(1-\beta_g^2)^{3/2}K(t), \quad (5)$$

where $K(t) = \int_0^t \kappa dt'$. If we assume that the EM field is constant, then $K(t) = \kappa t$, and for $t\to\infty$ only the term with $\ln(\beta_g - \beta)$ survives. In this limit we have

$$\beta = \beta_g - \exp[-\beta_g(1-\beta_g^2)^{3/2}\kappa t]. \quad (6)$$

We see that the maximum ion velocity approaches but never exceeds the group velocity of the laser.

Figure 1 shows the numerical solution of Eq. (3) for a Gaussian pulse, with duration $\tau = 27$ fs (10 cycles), wavelength $\lambda = 800$ nm, focal spot of $w_0 = 0.9\lambda$, which corresponds to an f number of $f/D = 1$, interacting with a 0.25λ thick hydrogen foil with the electron density of $n_e = 400 n_{\rm cr}$. The evolution of the maximum ion energy is shown in Fig. 1 for three different values of averaged laser pulse power [0.55 PW ($a = 248$), 1.1 PW ($a = 351$), and 1.8 PW ($a = 444$)] and two values of the group velocity, $\beta_g = 1$ and $\beta_g = 0.969$ ($\gamma_g \approx 4$, $w_0 = 0.9\lambda$, $f/D = 1$ [22]). For $P = 0.55$ PW, the ion energy dependences are very similar, since $\mathcal{F}_L/n_e l < \gamma_g - 1$; *i.e.*, the maximum achievable ion velocity is less than the laser group velocity, and the effects of group velocity are small. In two other cases ($P = 1.1$ PW and $P = 1.8$ PW), $\mathcal{F}_L/n_e l > \gamma_g - 1$, leading to significant differences between the cases of $\beta_g = 1$ and $\beta_g = 0.969$. While ($\beta_g = 1$) curves continue to grow, ($\beta_g < 1$) curves are limited by $\gamma_g - 1$. Thus, these cases demonstrate the constraint on maximum ion energy due to

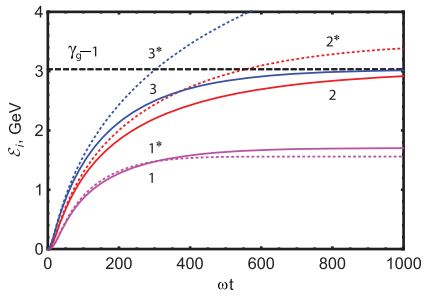

FIG. 1 (color online). The dependencies of the ion kinetic energy on time in the case of $\beta_g = 0.969$ (solid curves) and $\beta_g = 1$ (dashed curves) for three different values of the laser power, $P = 0.55$ PW(1), $P = 1.1$ PW(2), and $P = 1.8$ PW(3). The density of the foil is $n_e = 400n_{cr}$, and the thickness is $l = 0.25\lambda$. The laser pulse duration is 27 fs, and the f number is $f/D = 1$.

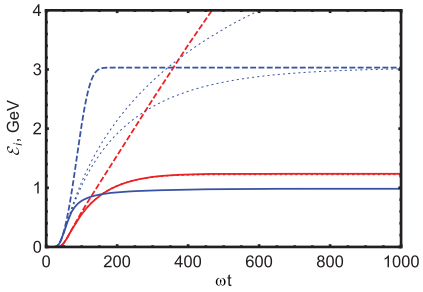

FIG. 2 (color online). The dependencies of the ion kinetic energy on time in cases of transverse expansion and laser divergence taken into account (solid curves), not taken into account [dotted curves, $\beta_g = 1$ (upper) and $\beta_g < 1$ (lower)], and the guided laser with $|\rho| = 1$ (dashed curves) for $f/D = 1$ (blue) and $f/D = 2$ (red). Laser pulse power is 1.8 PW, duration is 27 fs, the foil thickness is 0.25λ, and density is $n_e = 400n_{cr}$.

the laser group velocity being smaller than the vacuum light speed.

A group velocity smaller than the vacuum light speed appears naturally in the case of tightly focused laser pulses [1], which diverge rather quickly after passing through the focus. Assuming that this divergence forces the irradiated part of the foil to expand, following the increase of the laser spot size, we study how the transverse expansion of the target limits the maximum attainable ion energy during the RPA, and whether this limitation dominates over the fundamental effects of the group velocity. Assuming that the field of the pulse can be given by the paraxial approximation, characterized by the laser pulse waist at focus w_0 and the Rayleigh length $L_R = \pi w_0^2/\lambda$, the evolution of the laser pulse waist as it travels away from focus is $w(x) = w_0[1 + (x/L_R)^2]^{1/2}$, the amplitude of the field scales with the distance from the focus as $a(x) = a_0[1 + (x/L_R)^2]^{-1/2}$, and the group velocity is $\beta_g \simeq 1 - 1/k^2w_0^2$ [22]. Since we are interested in the maximum ion energy, we consider RPA of an on-axis element of the foil. The intensity profile near the axis can be approximated by an expanding spherical cup with curvature radius equal to the laser waist $w(x)$. The on-axis element of the foil can also be approximated by an expanding spherical cup with the curvature $w(x)$ and areal density equal to $n_e l = n_0 l_0[1 + (x/L_R)^2]^{-1}$ and $\varepsilon_e(x) = \varepsilon_e(0)[1 + (x/L_R)^2]^{-1}$. Substituting the field and areal density into Eq. (3), we see that the right-hand side of Eq. (3) depends on the distance from the focus only through the reflection coefficient [19]: $\rho(x) = [\gamma\varepsilon_e(x)/a(x)][R/(R+2)]^{1/2}$, where $R = [(a(x)^2 - \gamma^2\varepsilon_e(x)^2 - 1)^2 + 4a(x)^2]^{1/2} + a(x)^2 - \gamma^2\varepsilon_e(x)^2 - 1$.

In what follows, we solve Eq. (3) numerically, taking into account transverse expansion of the foil and laser pulse divergence. The evolution of the maximum ion energy is shown in Fig. 2 for a 1.8 PW laser pulse interacting with a 0.25λ thick hydrogen foil with the density of $n_e = 400n_{cr}$ for two values of the f number, $f/D = 1$ and $f/D = 2$ (solid), corresponding to $\beta_g = 0.969$, $a = 444$ and $\beta_g = 0.992$, $a = 225$, respectively. In order to demonstrate the effect of transverse expansion and laser divergence, we show two curves with no target expansion and laser divergence, $\beta_g = 1$ and $\beta_g < 1$ (dotted), which are the same as curves 3 in Fig. 1. Thus, this effect significantly modifies the maximum ion energy by switching off the acceleration early. The utilization of an external guiding structure may relax the limits on maximum attainable ion energy. To model such interaction, we solve Eq. (3), assuming that the laser pulse is guided by a self-generated channel with the transverse size of $w_0 = 0.9\lambda$ ($f/D = 1$) and $w_0 = 1.8$ ($f/D = 2$), and the foil stays opaque for the pulse ($|\rho| = 1$). The solutions for such configuration are shown by dashed curves in Fig. 2. One can see that the external guiding structure significantly enhances the maximum attainable ion energy, which is now limited by the laser group velocity in such a structure. In principle, a composite target, consisting of a thin foil, followed by a near critical density slab, may provide an example of such guiding. The laser pulse will accelerate the irradiated part of the foil in the self-generated channel in the NCD plasma [23]. Though the foil density will drop due to the transverse expansion, the NCD plasma electrons being snowplowed by the pulse would provide an opaque density spike, which being pushed by the radiation pressure would drag the ions of the foil with it. Thus, such configuration is similar to the one considered above: the laser pulse is guided with no diffraction and although the density of ions decreases, the reflection coefficient is equal to 1.

In Figs. 3 and 4, we present the results of 2D particle-in-cell (PIC) simulations (using the code REMP [24]), which indicate that, for the same laser pulse energy, the ion energy will be significantly higher in the case of a composite target than in the case of a single foil (the case of a single foil shows good agreement with the analytical results from Fig. 2, represented by the solid red line, and the foil becomes transparent for radiation at $\omega t \approx 250$). The maximum ion energy should be determined by the group velocity of the laser in the self-generated plasma channel; however, due to

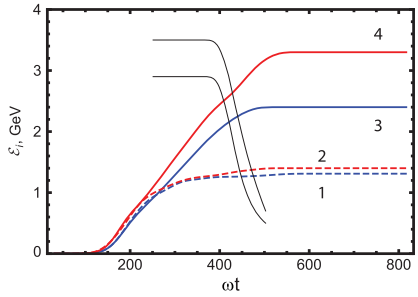

FIG. 3 (color online). The dependence of the ion energy on time for a composite target (solid curves) RPA and single foil (dashed curves) RPA. The simulation box is $100 \times 60\lambda^2$, $dx = dy = 0.025\lambda$, $dt = 0.0125 \times 2\pi/\omega$, and the number of particles per cell is 100. The Gaussian laser pulse is initialized at the left border with dimensionless potential $a_0 = 100$, waist $w = 4\lambda$, and duration $\tau = 27$ fs, which corresponds to the average power of 1.8 PW. The pulse is focused at the left front side of the target, which is placed 16λ away from the left border. The composite target consists of a fully ionized hydrogen foil and a hydrogen NCD plasma slab placed right behind the foil. The foil thickness is 0.25λ with densities $n_e = 400n_{\rm cr}$ (curves 1 and 3) and $n_e = 225n_{\rm cr}$ (curves 2 and 4). The thickness of the NCD plasma slab is 50λ and density is equal to $n_{\rm cr}$. The evolution of $\gamma_I - 1$ is shown by thin black curves for $n_e = 400n_{\rm cr}$ (lower curve) and $n_e = 225n_{\rm cr}$ (upper curve).

the fast depletion of the pulse as well as its reflection at the laser-plasma interface, the laser group velocity cannot unambiguously be determined from the results of PIC simulations. In this case, we chose the velocity of the laser-plasma interface β_I as the characteristic quantity for ion acceleration in the channel. Using results of Ref. [25], we can find the normalized velocity laser-plasma interface from the condition that it takes the depletion energy time $t_{\rm depl}$ for the laser pulse tail to reach the laser-plasma interface. This yields $\beta_I = \beta_g(1 - n_e/n_{\rm cr}a) \approx \beta_g(1 - 1/\gamma_g^2) = \beta_g^3$, *i.e.*, $\gamma_I \approx \gamma_g/3^{1/2} \approx 5$, which is in good agreement with the results of PIC simulations, taking into account pulse reflection during the initial interaction with the foil.

In Fig. 3, the energy $\gamma_I - 1$ (from PIC results) is shown by thin black curves. Note that $\gamma_I - 1$ remains constant during the pulse propagation through the NCD plasma, but after the pulse depletion becomes significant, it decreases, marking the end of the ion acceleration for both values of the foil density studied in simulations. We note that the ion energy is not able to reach the maximum value of $\gamma_I - 1$ due to the laser pulse depletion in the NCD plasma. In Fig. 4, the evolution of the proton density and spectrum are shown for the composite target (for single foil see Ref. [26]). We note that the electron heating can result in the transverse expansion of the foil [16]. However, for the laser target interaction parameters used in our simulations, the characteristic transverse temperature is approximately 3 times lower than the quivering energy of electrons in the transverse EM field.

In conclusion, we identified two factors that limit the maximum attainable in the RPA ion energy: (i) the fundamental effect of the laser pulse group velocity being less than vacuum light speed, and (ii) the transverse expansion of the target, which plays a major role when tightly focused pulses are used.

We showed that the utilization of external guiding may relax the constraints on maximum attainable ion energy. Namely, we used a composite target, a thin foil followed by an NCD slab. The NCD slab provided guiding of the laser pulse during the acceleration process. The comparison of a single foil RPA and a composite target RPA shows that, in the latter case, the ions have energy several times larger than in the former case, thus greatly increasing the effectiveness of the RPA regime of laser-driven ion acceleration. In such a configuration, the group velocity effects begin to dominate and determine the maximum achievable ion energy.

We acknowledge support from the NSF under Grant No. PHY-0935197 and the Office of Science of the US

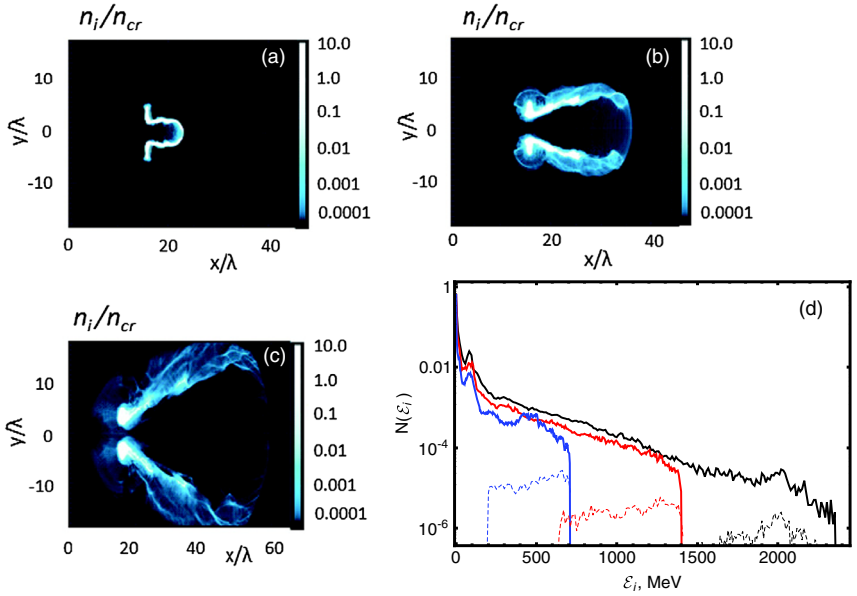

FIG. 4 (color online). The evolution of the density of the ions originating from the foil during the laser pulse interaction with a composite target. (a) $\omega t = 2\pi \times 35$, (b) $\omega t = 2\pi \times 50$, (c) $\omega t = 2\pi \times 75$, and (d) the evolution of the spectrum of ions originating from the foil: $\omega t = 2\pi \times 35$ (red curve), $\omega t = 2\pi \times 50$ (blue curve), and $\omega t = 2\pi \times 75$ (black curve). The dashed curves correspond to the ions accelerated inside a 10° angle and having low energy cut at 200, 650, and 1500 MeV, respectively. The parameters of the interaction are the same as in Fig. 3.

DOE under Contracts No. DE-AC02-05CH11231 and No. DE-FG02-12ER41798 and Ministry of Education, Youth, and Sports of the Czech Republic under the Project No. CZ.1.05/1.1.00/02.0061. The authors would like to thank C. Benedetti, M. Chen, C. G. R. Geddes, and L. Yu for discussions.

[1] E. Esarey, C. B. Schroeder, and W. P. Leemans, Rev. Mod. Phys. **81**, 1229 (2009).

[2] *ELI—Extreme Light Infrastructure Science and Technology with Ultra-Intense Lasers, Whitebook*, edited by G. A. Mourou, G. Korn, W. Sandner, and J. L. Collier (THOSS Media GmbH, Berlin, 2011).

[3] G. Mourou, T. Tajima, and S. V. Bulanov, Rev. Mod. Phys. **78**, 309 (2006); H. Daido, M. Nishiuchi, and A. S. Pirozhkov, Rep. Prog. Phys. **75**, 056401 (2012); A. Macchi, M. Borghesi, and M. Passoni, Rev. Mod. Phys. **85**, 751 (2013).

[4] M. Roth, T. E. Cowan, M. H. Key, S. P. Hatchett, C. Brown, W. Fountain, J. Johnson, D. M. Pennington, R. A. Snavely, S. C. Wilks, K. Yasuike, H. Ruhl, F. Pegoraro, S. V. Bulanov, E. M. Campbell, M. D. Perry, and H. Powell, Phys. Rev. Lett. **86**, 436 (2001); V. Yu. Bychenkov, W. Rozmus, A. Maksimchuk, D. Umstadter, and C. E. Capjack, Plasma Phys. Rep. **27**, 1017 (2001); A. Macchi, A. Antonicci, S. Atzeni, D. Batani, F. Califano, F. Cornolti, J. J. Honrubia, T. V. Lisseikina, F. Pegoraro, and M. Temporal, Nucl. Fusion **43**, 362 (2003); J. J. Honrubia, J. C. Fernandez, M. Temporal, B. M. Hegelich, and J. Meyer-ter-Vehn, Phys. Plasmas **16**, 102701 (2009).

[5] S. V. Bulanov and V. S. Khoroshkov, Plasma Phys. Rep. **28**, 453 (2002); S. V. Bulanov, J. J. Wilkens, M. Molls, T. Zh. Esirkepov, G. Korn, G. Kraft, S. D. Kraft, and V. S. Khoroshkov, Usp. Fiz. Nauk **184**, 1265 (2014).[Phys. Usp. **57**, 1149 (2014)].

[6] M. Borghesi, J. Fuchs, S. V. Bulanov, A. J. Mackinnon, P. K. Patel, and M. Roth, Fusion Sci. Technol. **49**, 412 (2006).

[7] K. Krushelnick, E. L. Clark, R. Allott, F. N. Beg, C. N. Danson, A. Machacek, V. Malka, Z. Najmudin, D. Neely, P. A. Norreys, M. R. Salvati, M. I. K. Santala, M. Tatarakis, I. Watts, M. Zepf, and A. E. Dangor, IEEE Trans. Plasma Sci. **28**, 1110 (2000).

[8] M. Nishiuchi *et al.*, arXiv:1402.5729.

[9] T. Esirkepov, M. Borghesi, S. V. Bulanov, G. Mourou, and T. Tajima, Phys. Rev. Lett. **92**, 175003 (2004).

[10] O. Klimo, J. Psikal, J. Limpouch, and V. T. Tikhonchuk, Phys. Rev. ST Accel. Beams **11**, 031301 (2008); A. P. L. Robinson, M. Zepf, S. Kar, R. G. Evans, and C. Bellei, New J. Phys. **10**, 013021 (2008); B. Qiao, M. Zepf, M. Borghesi, and M. Geissler, Phys. Rev. Lett. **102**, 145002 (2009); X. Q. Yan, C. Lin, Z. M. Sheng, Z. Y. Guo, B. C. Liu, Y. R. Lu, J. X. Fang, and J. E. Chen, Phys. Rev. Lett. **103**, 135001 (2009); J.-L. Liu, M. Chen, J. Zheng, Z.-M. Sheng, and C.-S. Liu, Phys. Plasmas **20**, 063107 (2013).

[11] S. Kar, M. Borghesi, S. V. Bulanov, M. H. Key, T. V. Liseykina, A. Macchi, A. J. Mackinnon, P. K. Patel, L. Romagnani, A. Schiavi, and O. Willi, Phys. Rev. Lett., **100**, 225004 (2008); K. U. Akli *et al.*, Phys. Rev. Lett. **100**, 165002 (2008); A. Henig, S. Steinke, M. Schnurer, T. Sokollik, R. Horlein, D. Kiefer, D. Jung, J. Schreiber, B. M. Hegelich, X. Q. Yan, J. Meyer-ter-Vehn, T. Tajima, P. V. Nickles, W. Sandner, and D. Habs, Phys. Rev. Lett. **103**, 245003 (2009); C. A. J. Palmer, N. P. Dover, I. Pogorelsky, M. Babzien, G. I. Dudnikova, M. Ispiriyan, M. N. Polyanskiy, J. Schreiber, P. Shkolnikov, V. Yakimenko, and Z. Najmudin, Phys. Rev. Lett. **106**, 014801 (2011); S. Kar, K. F. Kakolee, B. Qiao, A. Macchi, M. Cerchez, D. Doria, M. Geissler, P. McKenna, D. Neely, J. Osterholz, R. Prasad, K. Quinn, B. Ramakrishna, G. Sarri, O. Willi, X. Y. Yuan, M. Zepf, and M. Borghesi, Phys. Rev. Lett. **109**, 185006 (2012); S. Steinke, P. Hilz, M. Schnurer, G. Priebe, J. Branzel, F. Abicht, D. Kiefer, C. Kreuzer, T. Ostermayr, J. Schreiber, A. A. Andreev, T. P. Yu, A. Pukhov, and W. Sandner, Phys. Rev. ST Accel. Beams **16**, 011303 (2013); I. J. Kim, K. H. Pae, C. M. Kim, H. T. Kim, J. H. Sung, S. K. Lee, T. J. Yu, I. W. Choi, C.-L. Lee, K. H. Nam, P. V. Nickles, T. M. Jeong, and J. Lee, Phys. Rev. Lett. **111**, 165003 (2013).

[12] S. V. Bulanov, T. Zh. Esirkepov, M. Kando, A. S. Pirozhkov, and N. N. Rosanov, Usp. Fiz. Nauk **183**, 449 (2013).[Phys. Usp. **56**, 429 (2013)].

[13] S. Wilks, W. Kruer, M. Tabak, and A. B. Langdon, Phys. Rev. Lett. **69**, 1383 (1992); N. M. Naumova, T. Schlegel, V. T. Tikhonchuk, C. Labaune, I. V. Sokolov, and G. Mourou, Phys. Rev. Lett. **102**, 025002 (2009).

[14] S. V. Bulanov, T. Zh. Esirkepov, M. Kando, F. Pegoraro, S. S. Bulanov, C. G. R. Geddes, C. B. Schroeder, E. Esarey, and W. Leemans, Phys. Plasmas **19**, 103105 (2012).

[15] A. Einstein, Ann. Phys. (Leipzig) **17**, 891 (1905).

[16] F. Dollar, C. Zulick, A. G. R. Thomas, V. Chvykov, J. Davis, G. Kalinchenko, T. Matsuoka, C. McGuffey, G. M. Petrov, L. Willingale, V. Yanovsky, A. Maksimchuk, and K. Krushelnick, Phys. Rev. Lett. **108**, 175005 (2012).

[17] A. Macchi, S. Veghini, and F. Pegoraro, Phys. Rev. Lett. **103**, 085003 (2009); A. Macchi, S. Veghini, T. V. Liseylina, and F. Pegoraro, New J. Phys. **12**, 045013 (2010).

[18] S. V. Bulanov, E. Yu. Echkina, T. Zh. Esirkepov, I. N. Inovenkov, M. Kando, F. Pegoraro, and G. Korn, Phys. Rev. Lett. **104**, 135003 (2010).

[19] S. S. Bulanov, C. B. Schroeder, E. Esarey, and W. P. Leemans, Phys. Plasmas **19**, 093112 (2012).

[20] A. Sgattoni, P. Londrillo, A. Macchi, and M. Passoni, Phys. Rev. E **85**, 036405 (2012).

[21] V. A. Vshivkov, N. M. Naumova, F. Pegoraro, and S. V. Bulanov, Phys. Plasmas **5**, 2727 (1998).

[22] E. Esarey, P. Sprangle, M. Pilloff, and J. Krall, J. Opt. Soc. Am. B **12**, 1695 (1995).

[23] S. S. Bulanov, V. Yu. Bychenkov, V. Chvykov, G. Kalinchenko, D. W. Litzenberg, T. Matsuoka, A. G. R. Thomas, L. Willingale, V. Yanovsky, K. Krushelnick, and A. Maksimchuck, Phys. Plasmas **17**, 043105 (2010).

[24] T. Zh. Esirkepov, Comput. Phys. Commun. **135**, 144 (2001).

[25] S. V. Bulanov, I. N. Inovenkov, V. I. Kirsanov, N. M. Naumova, and A. S. Sakharov, Phys. Fluids B **4**, 1935 (1992); S. V. Bulanov, I. N. Inovenkov, V. I. Kirsanov, N. M. Naumova, A. S. Sakharov, and H. A. Shakh, Phys. Scr. **47**, 209 (1993); C. D. Decker, W. B. Mori, K. C. Tzeng, and T. Katsouleas, Phys. Plasmas **3**, 2047 (1996).

[26] See Supplemental Material at http://link.aps.org/supplemental/10.1103/PhysRevLett.114.105003, where ion density distribution and spectrum in the case of a single foil are shown.